AIP | Journal of Applied Physics

A comparative study of the magnetocaloric effect in RNi2 (R = Nd,Gd,Tb) intermetallic compounds

E. J. R. Plaza, V. S. R. de Sousa, P. J. von Ranke, A. M. Gomes, D. L. Rocco et al.

Citation: J. Appl. Phys. **105**, 013903 (2009); doi: 10.1063/1.3054178
View online: http://dx.doi.org/10.1063/1.3054178
View Table of Contents: http://jap.aip.org/resource/1/JAPIAU/v105/i1
Published by the AIP Publishing LLC.

A comparative study of the magnetocaloric effect in RNi_2 (R=Nd,Gd,Tb) intermetallic compounds

E. J. R. Plaza,[1,2,a)] V. S. R. de Sousa,[1] P. J. von Ranke,[1] A. M. Gomes,[3] D. L. Rocco,[4,5] J. V. Leitão,[4] and M. S. Reis[4]
[1]*Instituto de Física, Universidade do Estado do Rio de Janeiro (UERJ), Rua São Francisco Xavier 524, 20550-013 Rio de Janeiro, Brazil*
[2]*Instituto de Física "Gleb Wataghin," Universidade Estadual de Campinas (UNICAMP), 13083-970 Campinas, SP, Brazil*
[3]*Instituto de Física, Universidade Federal do Rio de Janeiro, CP 68528, 21941-972 Rio de Janeiro, Brazil*
[4]*CICECO, Universidade de Aveiro, 3810-193 Aveiro, Portugal*
[5]*Departamento de Física, Campus Morro do Cruzeiro, Universidade Federal de Ouro Preto, 35400-000 Ouro Preto, MG, Brazil*

(Received 10 June 2008; accepted 11 November 2008; published online 5 January 2009)

Conventional and anisotropic magnetocaloric effects were studied in cubic rare earth RNi_2 (R=Nd,Gd,Tb) ferromagnetic intermetallic compounds. These three compounds are representative of small, null, and large magnetocrystalline anisotropy in the series, respectively. Magnetic measurements were performed in polycrystalline samples in order to obtain the isothermal magnetocaloric data, which were confronted with theoretical results based on mean field calculations. For the R=Tb case, we explore the crystalline electrical-field anisotropy to predict the anisotropic magnetocaloric behavior due to the rotation of an applied magnetic field of constant intensity. Our results suggest the possibility of using both conventional and anisotropic magnetic entropy changes to extend the range of temperatures for use in the magnetocaloric effect. © *2009 American Institute of Physics*. [DOI: 10.1063/1.3054178]

I. INTRODUCTION

The recent discovery of a giant magnetocaloric effect (MCE) in the $Gd_5(Si_xGe_{1-x})_4$ system[1,2] has stimulated many experimental and theoretical studies on this subject. The Gd compounds are of particular importance due to their large magnetic moment and the negligible crystalline electrical field (CEF) quenching of the semifilled $4f$ shell of the Gd ion. When the magnetic moment of the magnetic ions presents practically only spin component, as is the case of Gd, the magnetic anisotropy due to the CEF can be neglected. On the other hand, CEF-anisotropy effects resulting from the coupling between magnetic interactions and the crystal lattice can be important in some magnetocaloric compounds. The conventional MCE is usually measured by the sample adiabatic temperature change ΔT (or isothermal entropy change ΔS) upon magnetic field intensity variation $\Delta H=H_f-H_i$ (H_f and H_i being the final and initial fields, respectively). However, in single-crystal magnetic materials, when the magnetization dependence on the magnetic field direction is relevant (i.e., the magnetic anisotropy is present), it is convenient to define ΔT (or ΔS) for a relative rotation of the applied magnetic field (of constant intensity) from one to another nonequivalent crystallographic direction.

In anisotropic magnetic materials, one can consider the easy and noneasy magnetic directions where the magnetization presents maximum and minimum values, respectively. The easy magnetic direction may depend on external parameters as is the case of the $NdAl_2$ and $HoAl_2$ ferromagnetic compounds which present a rotation of the easy magnetic direction when the magnetic field applied initially along a noneasy magnetic direction reaches a critical value.[3,4] Also, for a fixed magnetic field intensity, pointing in a noneasy direction, a temperature-induced spin reorientation signature can be expected as that observed in the MCE of the $DyAl_2$ compound.[5,6] Besides the RAl_2 system, other lanthanide compounds that can include spin reorientation are the RNi_2 compounds due to the interplay between magnetic interactions and the CEF.

From the technological point of view, the RNi_2 series, as well as the RAl_2 and their composites,[7] offers potential compounds for use as an active magnetic regenerator. For instance, appropriate molar combination of composites can be selected in order to obtain an approximated constant value for the ΔS versus T curves. This is very convenient for a range of the operation temperatures in the scope of the Ericsson cycle. Concerning this, it has been recently proposed the concomitant use of the anisotropic MCE together with the conventional one in order to extend the temperature range of magnetic refrigeration.[8,9] Therefore, the MCE characterization of anisotropic magnetic materials is very important.

In this paper, we report a comparative study about the conventional and anisotropic MCEs in some RNi_2 compounds (R=Nd,Gd,Tb). For this series, the selected rare-earth elements are representative of small, null, and large magnetic anisotropy that comes from the CEF. Magnetic measurements were performed in polycrystalline samples which were used to obtain the isothermal magnetocaloric potential through the use of the Maxwell's relation. By

a)Author to whom correspondence should be addressed. Electronic mail: plaza@ifi.unicamp.br.

means of calculations in the molecular field approximation including CEF effects, we obtained this same quantity in order to compare it with the experimental results. We also calculated the adiabatic temperature change and performed the statistical average considering the three main crystallographic directions to simulate the polycrystalline material. For the $TbNi_2$ compound, we highlighted the anisotropic behavior and predicted the magnetocaloric behavior due to a rotating magnetic field of constant intensity.

II. EXPERIMENTAL

Polycrystalline RNi_2 (R=Nd, Gd, and Tb) samples were prepared by arc melting in a purified argon atmosphere starting from the appropriate amounts of the constituent elements (99.9% pure for all the rare earths and 99.995% pure for the Ni). No weight loss was observed after the fusion. In order to ensure homogeneity, the ingots were sealed in evacuated quartz tubes and underwent heat treatment for 14 days at 900 K. The samples were characterized by x-ray diffraction and Rietveld refinements revealed that the samples belong to the space group $N°$ 216. Magnetic measurements were performed in a vibrating-sample magnetometer and commercial physical properties measurement system magnetometer in the field and temperature ranges of interest. We obtained $\Delta S_{\mathrm{mag}}(T)$ versus temperature curves from the experimental magnetization isothermals $M(H)$ through the use of the standard Maxwell relation.

III. THEORY

The RNi_2 compounds crystallize in the cubic Laves phase structure (or in a derived superstructure[10]) and their magnetism comes from the $4f$ unfilled R-shell since the Ni ions are practically nonmagnetic. However, the Ni ions contribute with conduction electrons which lead to indirect exchange interactions among the localized R-magnetic moments. Besides the exchange interaction usually considered in the molecular field approximation, the coupling of magnetic ions with the external magnetic field (the Zeeman interaction) and the cubic CEF constitutes an appropriated framework to describe the magnetic behavior of the RNi_2 compounds.[11] Therefore our model magnetic Hamiltonian can be written as

$$\hat{H} = -g\mu_B(\vec{H}+\lambda\vec{M})\cdot\vec{J} + W\left[\frac{X}{F_4}(O_4^0+5O_4^4) + \frac{(1-|X|)}{F_6}(O_6^0-21O_6^4)\right]. \quad (1)$$

Here, g is the Landé factor, μ_B is the Bohr magneton, $\vec{H}$ is the applied magnetic field, $\vec{M}$ is the magnetization, λ is the exchange parameter, and $\vec{J}$ is the total angular momentum vector operator. The CEF operator is written in the Lea *et al.*[12] representation, where F_4 and F_6 are dimensionless constants tabulated for each R-element, W gives the CEF energy scale, and X ($-1\leq X\leq 1$) gives the relative contributions of the fourth and sixth degrees in the O_n^m Stevens[13] equivalent operators. In order to investigate the magnetic anisotropy it is convenient to write

$$(\vec{H}+\lambda\vec{M})\cdot\vec{J} = [(H\cos\alpha+\lambda M_x)J_x + (H\cos\beta+\lambda M_y)J_y + (H\cos\gamma+\lambda M_z)J_z], \quad (2)$$

where α, β, and γ are the angles formed between the magnetic field vector and the x, y, and z crystallographic axes chosen as the [100], [010], and [001] crystallographic cubic directions, respectively.

The δ-component ($\delta=x,y,z$) of the magnetization vector is obtained by the thermodynamic average

$$M_\delta = g\mu_B \frac{\sum_{n=1}^{2J+1}\langle n|\hat{J}_\delta|n\rangle e^{-\varepsilon_n/k_BT}}{\sum_{n=1}^{2J+1} e^{-\varepsilon_n/k_BT}}, \quad (3)$$

where ε_n and $|n\rangle$ are the energy eigenvalues and eigenvectors of the Hamiltonian (1), respectively. With the set of Eqs. (1)–(3) the components of the magnetization for a selected direction of the applied magnetic field are obtained by means of self-consistent calculations. The intensity of the magnetization M and the component of the magnetization M_h along the applied magnetic field direction are $M=\sqrt{M_x^2+M_y^2+M_z^2}$ and $M_h=M_x\cos\alpha+M_y\cos\beta+M_z\cos\gamma$, respectively. Also, the directional (along the field direction) magnetic entropy of the magnetic system is given by

$$S_{\mathrm{mag}}^{\vec{H}} = R\left(\frac{1}{k_BT}\frac{\sum_{n=1}^{2J+1}\varepsilon_n e^{-\varepsilon_n/k_BT}}{\sum_{n=1}^{2J+1} e^{-\varepsilon_n/k_BT}} + \ln\sum_{n=1}^{2J+1} e^{-\varepsilon_n/k_BT}\right). \quad (4)$$

Besides the magnetic entropy given in Eq. (4), the lattice entropy S_{latt}, which is usually considered in the Debye approximation, and the electronic entropy S_{el} should be included in the total entropy for RNi_2 compounds. They are given by

$$S_{\mathrm{latt}} = -3R\ln\left[1-\exp\left(-\frac{\Theta}{T}\right)\right] + 12R\left(\frac{T}{\Theta}\right)^3\int_0^{\Theta/T}\frac{x^3dx}{\exp(x)-1}, \quad (5)$$

where Θ is the effective Debye temperature, and

$$S_{\mathrm{el}} = \bar{\gamma}T, \quad (6)$$

where $\bar{\gamma}$ is the Sommerfeld coefficient.

We use interpolated Θ-values from the nonmagnetic $LaNi_2$ and $LuNi_2$ compounds[14] and the common value $\bar{\gamma}=5.4$ mJ mol^{-1} K^{-2} for the studied RNi_2 compounds. Then, the total entropy is given by

$$S = S_{\mathrm{mag}} + S_{\mathrm{latt}} + S_{\mathrm{el}}. \quad (7)$$

Now, we consider the set $(\alpha_e,\beta_e,\gamma_e)$ as the angles of the easy magnetic direction in respect to the x, y, and z crystallographic axes and the set (α,β,γ) as the angles of a non-easy magnetic direction to select two magnetic field directions. Then, in general, the two thermodynamic potentials,

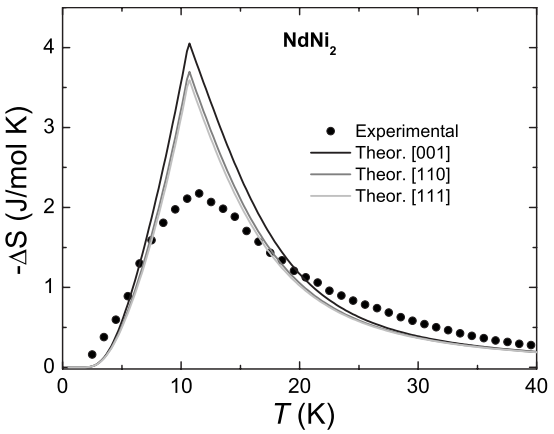

FIG. 1. Experimental and calculated directional components of magnetic entropy changes for $NdNi_2$ compound for the variation H: 0 to 5 T. Theoretical results correspond to calculations in the main crystallographic cubic axis: [001], [110], and [111] directions.

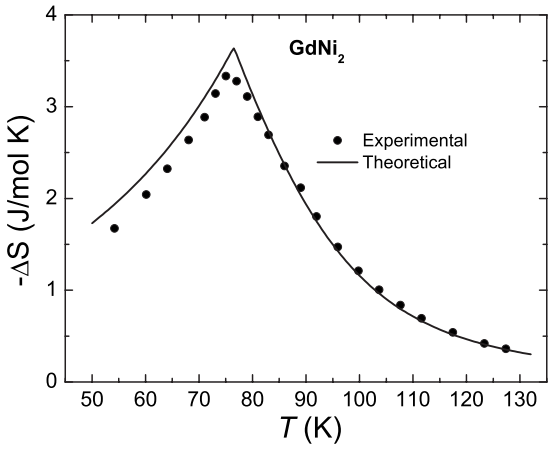

FIG. 2. Experimental and calculated magnetic entropy changes for $GdNi_2$ compound for magnetic field changes H: 0 to 5 T.

i.e., ΔS and ΔT, can be calculated using Eq. (7) in either case: (1) fixing the magnetic field direction and changing its intensity, which defines the conventional potentials $\Delta S(T) = S(T,H_f,\alpha,\beta,\gamma) - S(T,H_i,\alpha,\beta,\gamma)$ and $\Delta T(S) = T(S,H_f,\alpha,\beta,\gamma) - T(S,H_i,\alpha,\beta,\gamma)$, or (2) fixing the magnetic field intensity and changing its direction, which defines the anisotropic magnetocaloric potentials $\Delta S_{an}(T) = S(T,H,\alpha_e,\beta_e,\gamma_e) - S(T,H,\alpha,\beta,\gamma)$ and $\Delta T_{an}(S) = T(S,H,\alpha_e,\beta_e,\gamma_e) - T(S,H,\alpha,\beta,\gamma)$. In Sec. IV, we apply the above relations to study the specific aspects of the conventional and the anisotropic MCE in the $NdNi_2$, $GdNi_2$, and $TbNi_2$ compounds.

IV. RESULTS AND DISCUSSION

In order to perform our calculations, we considered the following magnetic model parameters: $W=0.28$ meV, $X=-0.89$, $\lambda=119$ T^2/meV for $NdNi_2$, $\lambda=93.5$ T^2/meV for $GdNi_2$, and $W=-0.066$ meV, $X=-0.73$, $\lambda=32$ T^2/meV for $TbNi_2$, as used in an earlier report.[15] The $NdNi_2$ orders ferromagnetically below 11 K with the easy axes along the $\langle 100\rangle$ directions. The $GdNi_2$ is isotropic and orders at $T_C=78$ K, whereas $TbNi_2$, the more anisotropic compound considered here, has $T_C=37.5$ K and easy axes along the $\langle 111\rangle$ directions. In all cases, the experimental and calculated directional components of the magnetic entropy change for the selected RNi_2 compounds are given for the magnetic field variation from 0 to 5 T.

The temperature dependence of the conventional isothermal magnetocaloric potential of polycrystalline $NdNi_2$ compound is presented in Fig. 1. It was evaluated indirectly by magnetic measurements through the Maxwell relation

$$-\Delta S(T) = S(T,H_i) - S(T,H_f) = \int_{H_i}^{H_f} -(\partial M/\partial T)_H dH, \quad (8)$$

since the lattice and electronic contributions to the total entropy can be considered independent from magnetic field in the RNi_2 series. Also, the above relation can be applied using magnetization calculations [by Eq. (3)] giving identical results as that obtained by Eq. (4). The theoretical results are also shown in Fig. 1, indicating the very small magnetic anisotropy in this case. The agreement between experimental and calculated results is satisfactory out of the region of the magnetic phase transition. Some inhomogeneities in the polycrystalline sample can enlarge and diminish the ΔS peak (in the transition region) due to the $\partial M/\partial T$ smoothing effect. It is important to emphasize that the experimental result comes from a polycrystalline sample and therefore that result corresponds to an average over all of the possible directions.

Figure 2 displays the experimental data and theoretical results of $-\Delta S$ for the $GdNi_2$ compound showing an excellent accordance. In this case an equivalent theoretical curve can be obtained using the well known Brillouin function for the magnetization and the Maxwell relation.

Also, the experimental data and theoretical results for the conventional MCE in $TbNi_2$ compound, characterized here by ΔS, are shown in Fig. 3. Theoretical results correspond to calculations in the main crystallographic cubic axes directions, namely, [001], [110], and [111], and the mean is taken as $(\Delta S^{[001]}+\Delta S^{[110]}+\Delta S^{[111]})/3$, which permit us the comparison with the experimental results. From comparison one observes an excellent agreement between our experimental data and calculation.

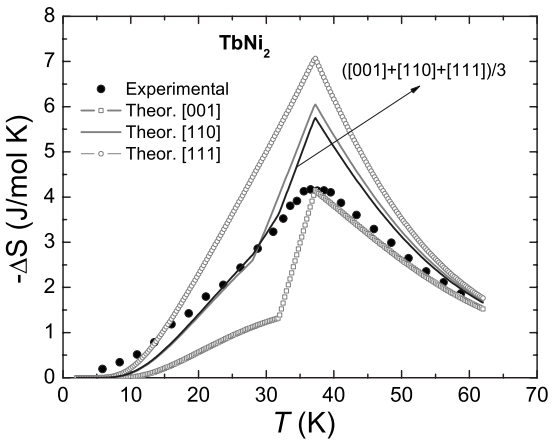

FIG. 3. Experimental and calculated directional components of magnetic entropy change for $TbNi_2$ compound for the magnetic field variation H: 0 to 5 T. Theoretical results correspond to calculations in the main crystallographic cubic axes: [001], [110], and [111] directions. The mean is taken as $(\Delta S^{[001]}+\Delta S^{[110]}+\Delta S^{[111]})/3$.

The $R\mathrm{Ni}_2$ compounds exhibit second order magnetic phase transitions. For NdNi_2 and TbNi_2 the CEF quenching of the magnetization is responsible for the corresponding low ΔS peak value at T_C. In spite of this quenching the conventional MCE peak for TbNi_2 is larger than that corresponding to GdNi_2 due to larger free saturation gJ value for Tb than that for Gd, $9\mu_B$, and $7\mu_B$, respectively.

The GdNi_2 compound is well described by the Brillouin function indicating the isotropic character of the magnetization without quenching effect in the saturation moment. This is not the case for the NdNi_2 compound in spite of the isotropic character of the MCE.

As observed in Fig. 3, the TbNi_2 compound shows high anisotropy when compared with NdNi_2 and presents the largest MCE in [111] direction, as indicated by the calculations. This is consistent with the easy axis along the [111] direction and the strong anisotropy due to CEF effect. The spin reorientation temperatures were obtained at $T_{\mathrm{SR}}=28$ and 32 K for the [110] and [001] applied magnetic field directions, respectively.

In the following, we will consider the anisotropic MCE for the TbNi_2 case. Setting the easy axis along the [111] direction one can investigate the influence of a magnetic field rotation from [111] to [001] direction on the MCE. For the case of $H=0$ and 5 T the calculated thermal evolution of M and M_h components for these directions is illustrated in Fig. 4(a). Evidently, for the [111] easy-axis direction one obtains $M=M_h$, whereas that is true along the [001] direction for temperatures above $T_{\mathrm{SR}}=32$ K. As one can note, the kink in the total magnetization at 5 T corresponds to an alignment ($M=M_{[001]}$ for $\vec{H}\|[001]$) and is associated to a spin-reorientation process that occurs continuously.

The corresponding anisotropic entropy change can be calculated directly according to $-\Delta S_{\mathrm{an}}=S^{[001]}-S^{[111]}$, where $S^{[111]}$ and $S^{[001]}$ are the directional entropies calculated directly from Eq. (4). Otherwise, through magnetization data one can obtain the usual MCE for those directions, i.e., $-\Delta S^{[111]}$ and $-\Delta S^{[001]}$ for a magnetic field variation from 0 to 5 T in such a way that $-\Delta S^{[111]}-(-\Delta S^{[001]})=S^{[001]}-S^{[111]}$ gives the anisotropic entropy change (for $H=5$ T). We display in Fig. 4(b) the obtained theoretical result for this case. The conventional $-\Delta S$ for a magnetic field variation from 0 to 5 T along the [001] direction was included for comparison. The corresponding adiabatic magnetocaloric potential is displayed in Fig. 4(c) and was obtained directly from the calculated entropies showed in the inset. It is interesting to note the appearance of the peaks in Figs. 4(a) and 4(b). In ferromagnets, caretlike peaks of conventional $-\Delta S$ and ΔT versus T curves are associated to the second order ferromagnetic-paramagnetic transition. One also observes caretlike peaks of anisotropic $-\Delta S_{\mathrm{an}}$ and ΔT_{an} versus T curves but in these cases, they are associated to a continuous spin reorientation. By increasing the temperature up to T_{SR} the rate of growth of $-\Delta S_{\mathrm{an}}$ (ΔT_{an}) is larger than that of $-\Delta S$ (ΔT). This occurs because the entropy $S^{[001]}$ ($\vec{H}\|[001]$) with $H=5$ T is very close to the entropy in the absence of field, whereas it is well away from $S^{[111]}$ ($\vec{H}\|[111]$) with $H=5$ T [$S^{[111]}$ (T) presents the maximum degree of magnetic order in comparison to other directions]. Note that above T_{SR} the opposite is verified and the signature of the spin reorientation is well defined as an abrupt change in growth in both $-\Delta S$ and ΔT versus T conventional curves.

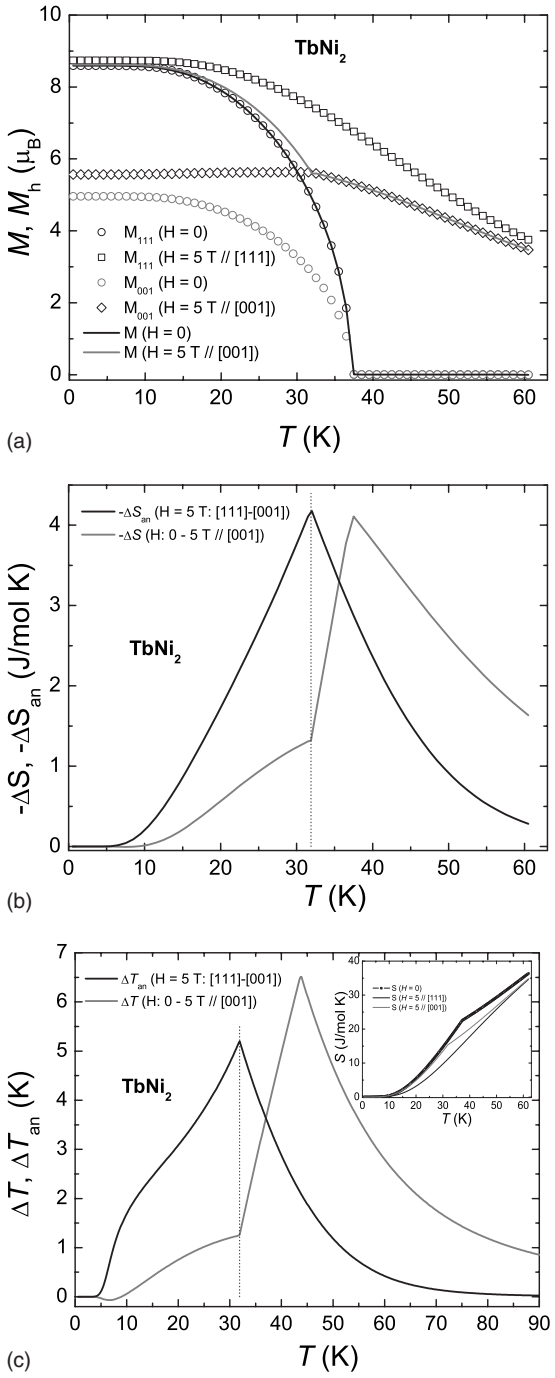

FIG. 4. (a) Calculated temperature dependence of the total magnetization M and their component along the field M_h (h: [111], [001]) for TbNi_2 compound with fields $H=0$ and 5 T. (b) Theoretical calculations for the conventional (H: from 0 to 5 T in the [001] direction) and anisotropic (for a [111] to [001] vector field variation in intensity 5 T) entropy changes. (c) Theoretical calculations for the conventional (H: from 0 to 5 T in the [001] direction) and anisotropic (for a [111] to [001] vector field variation in intensity 5 T) temperature changes obtained directly from S vs T curves shown in the inset.

V. CONCLUSION

In conclusion, we studied the conventional and anisotropic MCE in $R\mathrm{Ni}_2$ compounds (R=Nd, Gd, Tb). Theoreti-

cal considerations include the anisotropy that comes from the CEF interaction. For $GdNi_2$ and $NdNi_2$ there is a null or very weak anisotropy in comparison to that observed in $TbNi_2$ compound. For anisotropic $TbNi_2$ the explicit evolution of the entropy curves reveals the characteristics of the spin reorientation by the kinks in the $-\Delta S$ and ΔT curves. The maxima observed in the $-\Delta S_{an}$ and ΔT_{an} curves are associated to a spin reorientation that occurs continuously. The behavior of both curves suggests how to extend the range of temperatures for use in the MCE: subject of the anisotropic magnetic single crystal to a magnetic field along one axis followed by a rotation of the sample. This implies the use of materials in single crystalline form to explore both conventional and anisotropic MCEs. We hope this study can stimulate the synthesis and characterization of single crystals in this series as well as many others in order to check our predictions.

ACKNOWLEDGMENTS

The authors are grateful to Fundação de Amparo à Pesquisa do Estado de Rio de Janeiro (Faperj) and to Conselho Nacional de Desenvolvimento Científico e Tecnológico (CNPq) for the financial support. The authors also thank FCT for the VSM equipment (Grant No. REEQ/1126/2001). D.L.R. thanks CICECO for the grant.

[1] V. K. Pecharsky and K. A. Gschneidner, Jr., Phys. Rev. Lett. **78**, 4494 (1997).
[2] V. K. Pecharsky and K. A. Gschneidner, Jr., Appl. Phys. Lett. **70**, 3299 (1997).
[3] P. J. von Ranke, N. A. de Oliveira, C. Mello, D. C. Garcia, V. A. de Souza, and A. M. G. Carvalho, Phys. Rev. B **74**, 054425 (2006).
[4] I. G. de Oliveira, D. C. Garcia, and P. J. von Ranke, J. Appl. Phys. **102**, 073907 (2007).
[5] A. L. Lima, A. O. Tsokol, K. A. Gschneidner, Jr., V. K. Pecharsky, T. A. Lograsso, and D. L. Schlagel, Phys. Rev. B **72**, 024403 (2005).
[6] P. J. von Ranke, N. A. de Oliveira, D. C. Garcia, V. S. R. de Souza, V. A. de Souza, A. M. G. Carvalho, S. Gama, and M. S. Reis, Phys. Rev. B **75**, 184420 (2007).
[7] A. M. G. Carvalho, J. C. P. Campoy, A. A. Coelho, E. J. R. Plaza, S. Gama, and P. J. von Ranke, J. Appl. Phys. **97**, 083905 (2005).
[8] E. J. R. Plaza, V. S. R. de Sousa, B. P. Alho, and P. J. von Ranke (unpublished).
[9] P. J. von Ranke, N. A. de Oliveira, E. J. R. Plaza, V. S. R. de Souza, B. Alho, A. M. G. Carvalho, S. Gama, and M. S. Reis, J. Appl. Phys. **104**, 093906 (2008).
[10] A. Lindbaum, E. Gratz, and S. Heathman, Phys. Rev. B **65**, 134114 (2002).
[11] H. G. Purwins and A. Leson, Adv. Phys. **39**, 309 (1990).
[12] K. R. Lea, M. J. M. Leask, and W. P. Wolf, J. Phys. Chem. Solids **23**, 1381 (1962).
[13] K. W. H. Stevens, Proc. Phys. Soc., London, Sect. A **65**, 209 (1952).
[14] P. J. von Ranke, V. K. Pecharsky, and K. A. Gschneidner, Jr., Phys. Rev. B **58**, 12110 (1998).
[15] P. J. von Ranke, E. P. Nóbrega, I. G. de Oliveira, A. M. Gomes, and R. S. Sarthour, Phys. Rev. B **63**, 184406 (2001).